

ISTITUTO NAZIONALE DI FISICA NUCLEARE  
Laboratori Nazionali di Frascati

LNF-83/69(R)  
21 Ottobre 1983

D. Babusci, R. Bernabei, L. Casano, S. d'Angelo, M. P. De Pascale,  
S. Frullani, G. Giordano, B. Girolami, G. Matone, M. Mattioli, P.  
Picozza, D. Prospero and C. Schaerf: MEASUREMENT OF  
DEUTERON PHOTODISINTEGRATION ASYMMETRY AT  
 $E_\gamma = 19.8, 29.0$  AND  $38.6$  MeV

MEASUREMENT OF DEUTERON PHOTODISINTEGRATION ASYMMETRY AT  
 $E_\gamma = 19.8, 29.0$  AND  $38.6$  MeV

M. P. De Pascale, G. Giordano, G. Matone, P. Picozza  
INFN - Laboratori Nazionali di Frascati

D. Babusci, R. Bernabei, L. Casano, S. d'Angelo, M. Mattioli, D. Prosperi,  
C. Schaerf  
INFN - Sezione di Roma

S. Frullani, B. Girolami  
INFN - Sezione Sanità

Meson exchange currents (MEC) and isobar configurations (IC) in nuclei are recognized to play a very important role for a deeper description of nuclear dynamics, in particular at medium and short range regions<sup>(1, 2)</sup>. However, reliable calculations including break-up processes are at present available only for deuteron. This system, because loosely bound, gives extensive information about the  $\pi$ -MEC, effective at long range, but less about the intrinsic nucleon degrees of freedom, relevant in the short range regime<sup>(2)</sup>. Theoretical treatments<sup>(1-4)</sup>, supported by experimental measurements<sup>(5-8)</sup> show large MEC contributions in the deuteron photodisintegration, growing with increasing energy. Moreover, the angular dependence of the asymmetry parameter in this interaction results to be affected more than the total cross section by that part of MEC contributions not included in the Siegert operator.

We report preliminary results of measurements of the asymmetry parameter angular distribution in the deuteron photodisintegration at  $E_\gamma = 29.0$  and  $39.6$  MeV, together with some new results at  $E_\gamma = 19.8$  MeV<sup>(6)</sup>. The experiment has been performed at Frascati, using the monochromatic and linearly polarized  $\gamma$ -ray beam of the LADON facility<sup>(9)</sup>.

The center of mass differential cross section for the  $d(\vec{\gamma}, p)n$  process is expressed by the standard formula<sup>(10)</sup>:

$$\frac{d\sigma}{d\Omega} = I_0(\theta_n) + P I_1(\theta_n) \cos 2\varphi = I_0(\theta_n) [1 + P \Sigma(\theta_n) \cos 2\varphi], \quad (1)$$

where  $\theta_n$  is the c. m. angle between the neutron and the photon momenta and  $\varphi$  is the angle between the polarization and the reaction planes;  $P$  is the degree of linear polarization of the photon beam and

$$\Sigma(\theta_n) = \frac{I_1(\theta_n)}{I_0(\theta_n)} \quad (2)$$

is the asymmetry factor of the differential cross section.

By measuring the photoneutron yields at nine angles  $\theta_n$  and in series of alternate runs at  $\varphi = 0$  and  $\varphi = \pi/2$  under the same experimental conditions, we determined the angular distributions of  $I_0(\theta_n)$ ,  $I_1(\theta_n)$  and  $\Sigma(\theta_n)$ . An overall view of our experimental set-up is shown in Fig. 1.

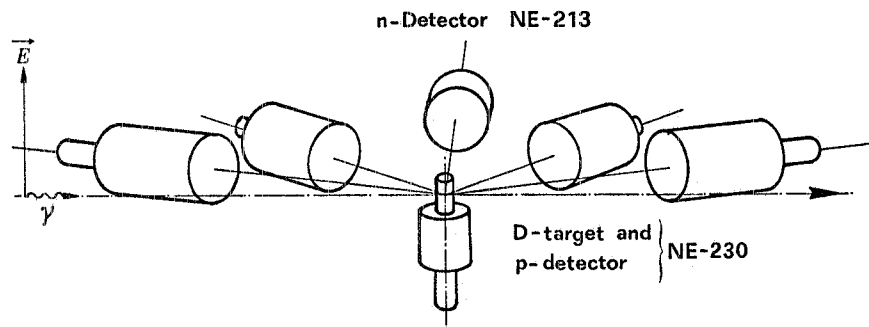


FIG. 1 - A schematic picture of the experimental set-up.

A 3.81 cm long NE-230 deuterated scintillator was used at the same time as deuterium target and proton energy detector. Five NE-213 liquid counters 30 cm diameter x x 15 cm long identified the photoneutrons by time of flight on a base of 130 cm. The  $\gamma$ -ray background was drastically reduced by pulse-shape discrimination in the target and in the neutron counters. Protons and neutrons were detected in coincidence with the electron bunch in the storage ring and the events recorded via Camac by a PDP11/34 minicomputer. The incident photon beam was  $\sim 99.8\%$  linearly polarized with an intensity of  $1 \sim 2 \times 10^5$   $\gamma$ /sec and 2-4% energy resolution. The flux was monitored by a lead glass counter and the energy spectrum checked by a magnetic pair spectrometer located before the target. The c. m. angles explored were:  $15^\circ$ ,  $30^\circ$ ,  $45^\circ$ ,  $60^\circ$ ,  $90^\circ$ ,  $120^\circ$ ,  $135^\circ$ ,  $150^\circ$ ,  $165^\circ$ .

From eq. (1) follows :

$$\frac{d\sigma}{d\Omega} = I_0(\theta_n) + PI_1(\theta_n) \quad \text{for } \varphi = 0 \quad , \quad (3)$$

$$\frac{d\sigma}{d\Omega} = I_0(\theta_n) - PI_1(\theta_n) \quad \text{for } \varphi = \frac{\pi}{2} \quad . \quad (4)$$

Then,  $I_0(\theta_n)$  and  $I_1(\theta_n)$  can be obtained from the experimental data by the expressions :

$$I_0(\theta_n) = \frac{\alpha}{2} \left[ K_1 Y(\theta_n, \varphi = 0) + K_2 Y(\theta_n, \varphi = \frac{\pi}{2}) \right] , \quad (5)$$

$$I_1(\theta_n) = \frac{\alpha}{2} P^{-1} \left[ K_1 Y(\theta_n, \varphi = 0) - K_2 Y(\theta_n, \varphi = \frac{\pi}{2}) \right] . \quad (6)$$

$Y(\theta_n, \varphi)$  is the ratio between the number of photoneutrons detected and the relative  $\gamma$ -ray flux;  $\alpha$  is a proportional constant. Finite solid-angle effects, neutron multiple scattering and absorption processes in the target are taken into account by the factors  $K_1$  and  $K_2$ , evaluated by a Monte Carlo calculation. Besides, by defining

$$R(\theta_n) = Y(\theta_n, \frac{\pi}{2})/Y(\theta_n, 0) \quad (7)$$

$\Sigma(\theta_n)$  can be expressed as :

$$\Sigma(\theta_n) = P^{-1} \frac{[1 - KR(\theta_n)]}{[1 + KR(\theta_n)]} \quad (8)$$

where  $K = K_2/K_1$ .

$I_0(\theta_n)$  and  $I_1(\theta_n)$  are shown in Figs. 2 and 4 for 19.8 and 29.0 MeV as a function of the neutron c. m. angle  $\theta_n$  and in unity of the total cross section for unpolarized  $\gamma$ -rays ( $\sigma_T = \int I_0(\theta_n, \varphi) d\Omega_n$ ).  $\Sigma(\theta_n)$  has been plotted in Figs. 3, 5 and 6 at the three energies explored. We notice that the results at  $E_\gamma = 38.6$  MeV are very preliminary.

Extensive theoretical calculations have been performed in the recent years on the parameter  $\Sigma$  and the differential cross section of the  $d(\vec{\gamma}, p)n$  process by Arenhövel<sup>(1, 2)</sup>, Cambi et al.<sup>(3, 11)</sup> and Rustgi and Vyas<sup>(4)</sup>.

In Figs. 2, 3, 4, 5 and 6 our data are compared with Cambi et al. results<sup>(11)</sup> obtained by using two different nucleon-nucleon potentials, the Reid soft-core (RSC) (dashed lines) and the De Tournelle-Sprung (version B) (DTS) (full lines). The Paris potential gives no appreciable difference with respect to RSC. Contributions associated with one pion exchange and  $\Delta$ -isobar excitation have been taken into account, in addition to the "normal" term under the Siegert hypothesis.

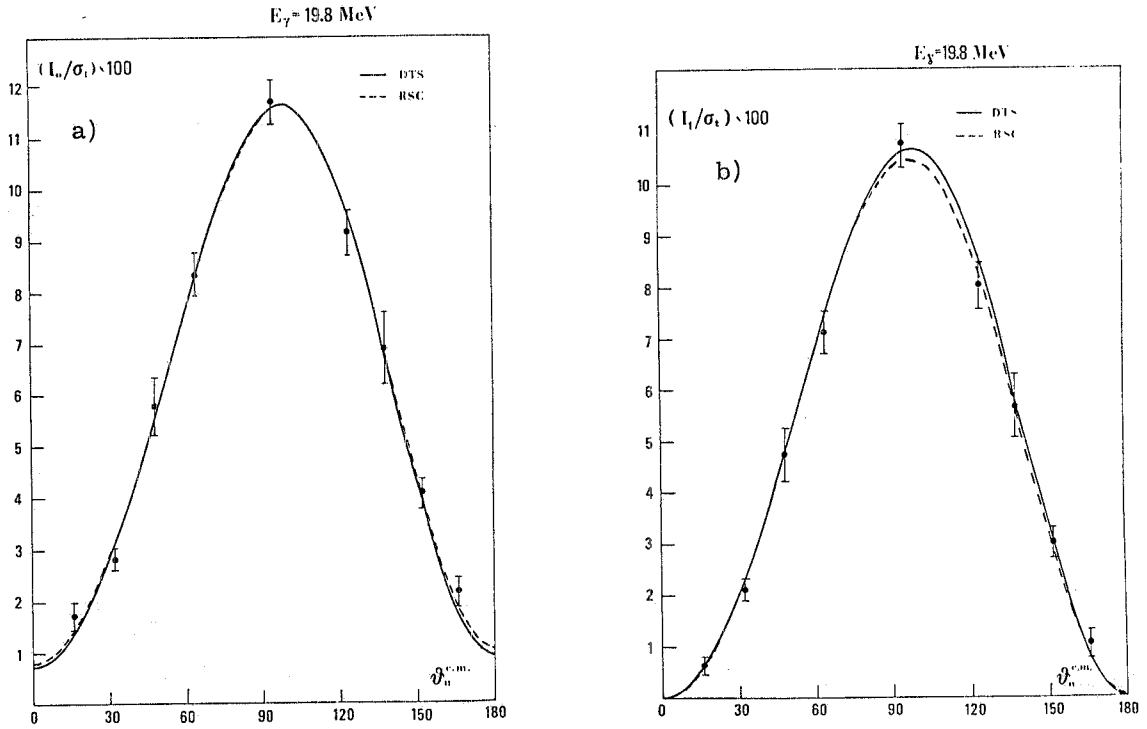


FIG. 2 - a)  $I_0(\theta_n)/\sigma_T$  versus  $\theta_n$  (c.m. neutron angle) for  $d(\vec{\gamma}, p)n$  at  $E_\gamma = 19.8$  MeV. Dashed and full curves are theoretical calculations from ref. (11) with RSC and DTS potentials. b) Same as a) for  $I_1(\theta_n)/\sigma_T$ .

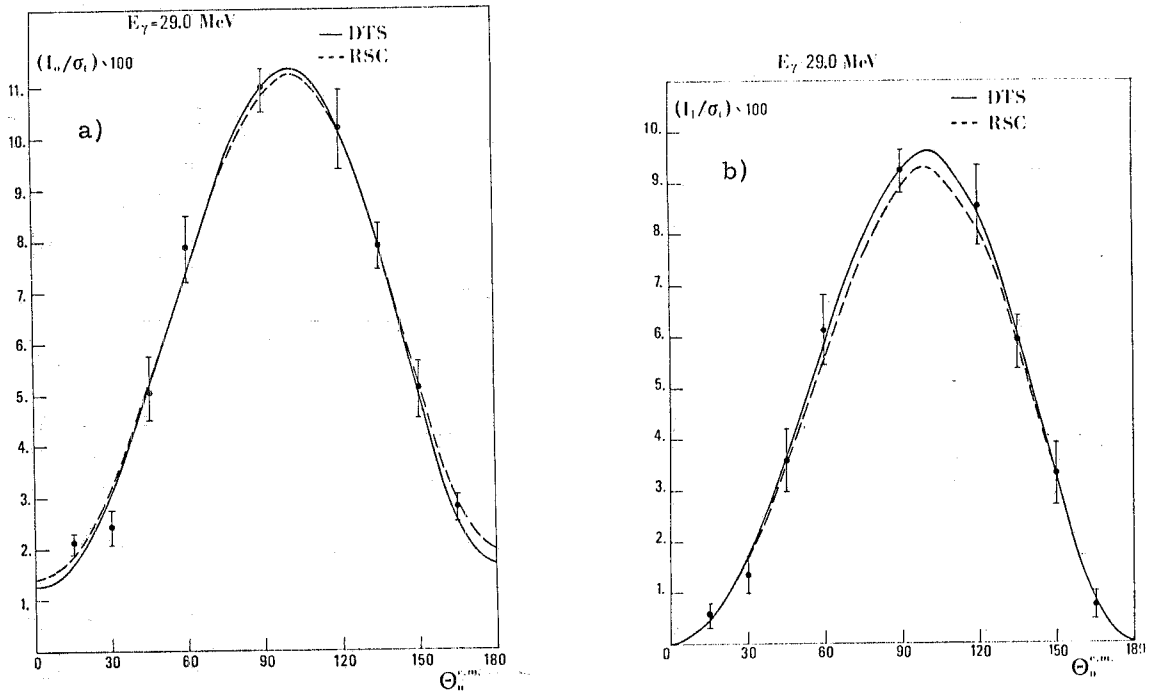


FIG. 4 - a)  $I_0(\theta_n)/\sigma_T$  versus  $\theta_n$  (c.m. neutron angle) for  $d(\vec{\gamma}, p)n$  at  $E_\gamma = 29.0$  MeV. Dashed and full curves are theoretical calculations from ref. (11) with RSC and DTS potentials. b) Same as a) for  $I_1(\theta_n)/\sigma_T$ .

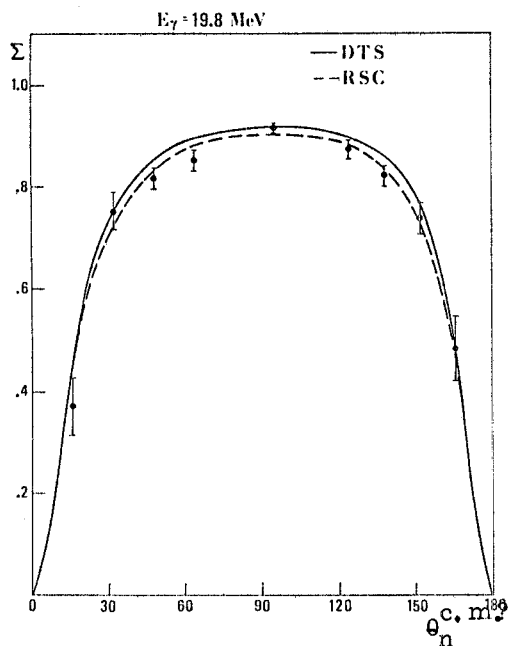


FIG. 3 - Same as Fig. 2 for  $\Sigma(\theta_n)$ .

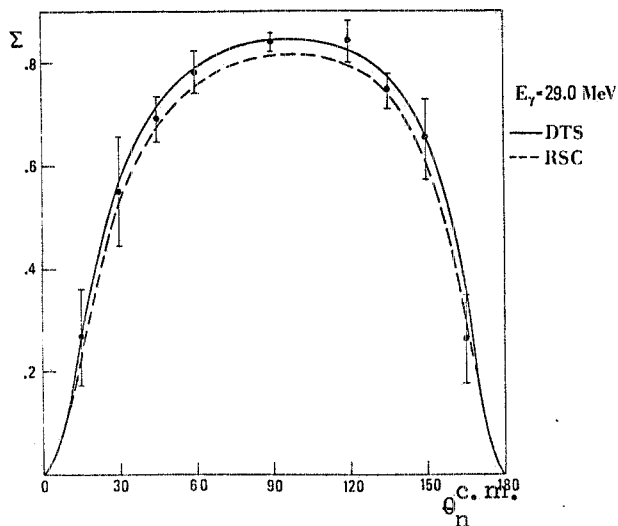


FIG. 5 - Same as Fig. 4 for  $\Sigma(\theta_n)$ .

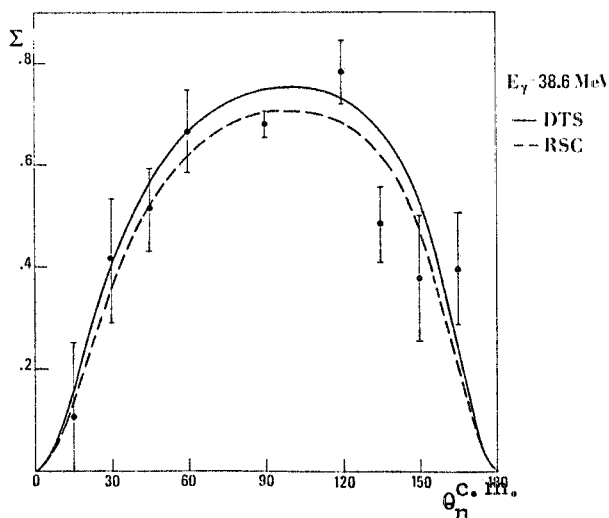


FIG. 6 -  $\Sigma(\theta_n)$  versus  $\theta_n$  (c.m. neutron angle) for  $d(\vec{\gamma}, p)n$  at  $E_\gamma = 38.6$  MeV. Dashed and full curves are theoretical calculations from ref. (11) with RSC and DTS potentials.

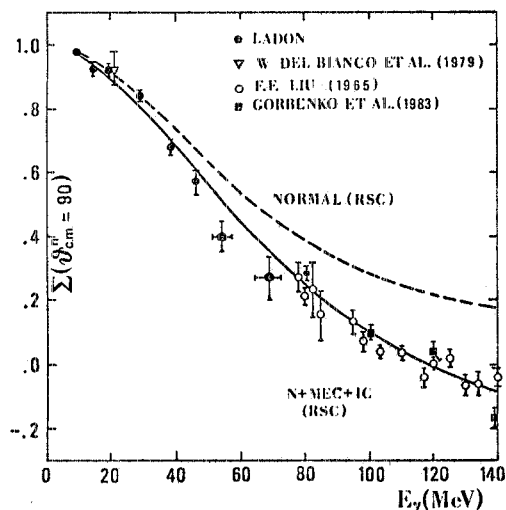


FIG. 7 -  $\Sigma(\theta_n)$  for  $d(\vec{\gamma}, p)n$  versus  $E_\gamma$  at  $\theta_n$  (c.m. neutron angle) =  $\pi/2$ . Dashed and full curves are Arenhövel calculations in "Normal" and N+MEC+IC approximations<sup>(2)</sup>.

A global analysis of our preliminary data in terms of  $I_0(\theta_n)$  and  $I_1(\theta_n)$  functions leads to a full compatibility with the theory developed using either of the two potentials. Therefore, an improved statistical accuracy and a complete study of single components determining  $I_0(\theta_n)$  and  $I_1(\theta_n)$  are necessary to become sensitive to potential effects, and to obtain definite information about the D-wave percentage in deuteron.

The effect of MEC contributions to the  $\Sigma(\theta_n)$  parameter, beyond the Siegert operator, is shown in Fig. 7, where our data are given in function of  $E_\gamma$  at  $\theta_n = \pi/2$ . Previous results of our group up to 70 MeV are also reported together with the Liu<sup>(7)</sup> and Gorbenko et al.<sup>(8)</sup> data at higher energies. The theoretical curve is an Arenh vel's<sup>(2)</sup> calculation performed using the Reid potential. The importance of the explicit "additional" term for the meson exchange currents is evident and increases with energy.

We would like to thank E. Cima, A. Dante, L. Ruggieri and E. Turri for their assistance during the experiment.

#### REFERENCES

- (1) - H. Arenh vel, in Proceedings of the Workshop on Intermediate Energy Nuclear Physics with Monochromatic and Polarized Photons, Frascati, July 1980, Ed. by G. Matone and S. Stipcich (Laboratori Nazionali di Frascati, 1980).
- (2) - H. Arenh vel, Nuovo Cimento 76A, 256 (1983).
- (3) - A. Cambi, B. Mosconi and P. Ricci, Phys. Rev. Letters 48, 462 (1982).
- (4) - M. L. Rustigi and R. Vyas, Phys. Letters 121B, 365 (1983).
- (5) - W. Del Bianco et al., Phys. Rev. Letters 47, 1118 (1981).
- (6) - M. P. De Pascale et al., Phys. Letters 114B, 11 (1982).
- (7) - F. F. Liu, Phys. Rev. 138B, 1443 (1965).
- (8) - V. G. Gorbenko et al., Nuclear Phys. A381, 330 (1982).
- (9) - L. Federici et al., Nuovo Cimento B59, 247 (1980).
- (10) - F. Partovi, Ann. of Phys. 27, 79 (1964).
- (11) - A. Cambi et al., private communication.